# IN-PLANE CYCLIC TESTS OF PLASTERED STRAW BALE WALL ASSEMBLIES

Cale Ash, Mark Aschheim
**University of Illinois**

David Mar
**Tipping-Mar + Associates**

**Abstract**

The construction and testing of six full-scale plastered straw bale wall assemblies is described in this report. The specimens consisted of three cement stucco skinned walls and three earth plaster skinned walls representing varying levels of reinforcement detailing. All walls were tested in-plane under either cyclic or monotonic lateral loadings. Measured behavior is presented in this report, along with recommendations for future work.

**Acknowledgements**

The authors of this report wish to express their sincere thanks to the following individuals and organizations: Ecological Building Network for securing project funding under the leadership of Bruce King. The Tides Center for administering the project and the California Department of Food & Agriculture for sponsoring the project. Tim Owens-Kennedy of Vital Systems for providing his expertise and the effort of Robin Slimmer, Tobias Hall, and David Stripling for wall construction. Jim Gambill and Bill Gordon of the United States Army Corps of Engineers Construction Engineering Research Laboratory in Champaign, IL for their expertise in setting up and running the tests. Chris Dunbar and Alex Pence for their helpful assistance in the laboratory. Special thanks to an ad-hoc group of self-proclaimed baleheads including Kevin Donahue, Tim Owens-Kennedy, Kelly Learner, and Dan Smith, for their assistance in developing the specimen designs and to David Mar and the staff of Tipping Mar and Associates for providing superb construction drawings.

**Table of Contents**

# 1. Introduction

## 1.1. Overview

This report presents the experimental results obtained from the in-plane cyclic tests of six load-bearing plastered straw ball wall assemblies. Six full-scale walls were tested: three had earth plaster skins and three had cement stucco skins, each with varied details. Five of the walls were tested under reversed cyclic loading to simulate their response to earthquake ground shaking. The remaining wall had details characteristic of non-seismic construction and was tested under monotonic loading.

## 1.2. Motivation

Despite over one hundred years of use as a building system, surprisingly little research and testing has been conducted to date on the performance of straw bale construction. This dearth of prior knowledge coupled with a renewed interest in sustainable construction practices led to the development of an organized set of engineering experiments intended to substantially increase the knowledge base of straw bale builders and engineers. The tests progress from small scale tests of components to medium scale tests of assemblies of components to large scale tests of entire wall assemblies (as reported herein).

## 1.3. Organization of Report

This report is divided into chapters describing all steps of the experimental project, from wall design and construction to testing and analysis of results. Chapter 2 describes the engineering principles that were applied in the design of the walls and their reinforcement details. The materials and techniques used in construction of the wall assemblies are described in Chapters 3 and 4. Chapter 5 describes the experimental testing sequence, including the protocol used for testing each wall. Test results from each wall specimen are presented in detail in Chapter 6 while comparisons between walls are made in Chapter 7. The conclusions and recommendations for future work made in Chapter 8 complete the report.

## 2. Idealized Wall Behavior

The straw bale wall assembly represents a composite of elements that work together to resist lateral and gravity forces. One of the basic tenets of earthquake resistant design is to provide a ductile mechanism of resistance to lateral forces. Because the forces "flow" through many individual elements, the provision of ductility requires that brittle elements be provided with sufficient strength to ensure that ductile behavior develops in those elements capable of ductile response. Figure 2.1 illustrates one conception of the flow of forces in a straw bale wall assembly. In this figure, lateral forces applied at the top of the wall are resisted by an internal truss, composed of diagonal compression struts within the plaster skins or the straw bales and tension developed in vertical and horizontal ties in the stucco or plaster skins. Although discrete forces are shown in the figure, the actual forces are understood to be distributed throughout the straw or plaster, or carried by the mesh or twine. For the force flows illustrated in the figure, ductility would be obtained by yielding of the mesh in tension or deformation of the straw bales in compression, provided that other elements have sufficient strength and stiffness to cause the deformations to concentrate in the mesh or the bales.

It is clear that earth plaster and stucco facings are much stiffer than the straw bales themselves, and so if the compression struts in the bales are to be fully mobilized, the facings would have to degrade significantly under previous load reversals. Prior to this degradation, stress will develop throughout the field of each face, and these stresses will redistribute as the facings crack or fail locally due to the development of principal tension and principal compression stresses due to the applied lateral and gravity loads. The best prospects for obtaining "ductile" seismic response appear to be associated with several alternative possibilities: (1) rocking of the wall, (2) flexural yielding of the wall, and (3) development of compression struts in the bales. Rocking of the wall is associated with the opening of a gap at the base of the wall. Tensile reinforcement, if present, will yield and then fracture. Gravity loads, consisting of wall self weight and any load applied at the top of the wall, will provide a restoring moment that resists rocking about the toe of the wall. Flexural yielding at the base of the wall relies upon tensile reinforcement to develop flexural resistance to the applied lateral force. Both flexural yielding and rocking require that the compression zone of the wall not fail and that the shear strength of the wall be adequate. Sources of deformation include flexural yielding, gap opening, and horizontal slip at the base of the wall. The development of a compression strut in the bales normally requires the facings to be heavily damaged or to spall off, while maintaining the integrity of reinforcement and the connections at the top and bottom of the wall.

One of the objectives of the small and medium scale tests done as part of this overall research program was to characterize the properties of the various elements that are mobilized in the load path of the wall assembly so that these components could be proportioned to obtain a ductile mechanism. The large scale wall assembly tests are intended to verify the ability of the designs to provide ductile behavior and to establish the degree of detailing required to achieve a desired level of ductility, or more generally, to determine the effect of various levels of detailing on the ductile behavior of entire wall assemblies.

The lightly detailed specimens, Walls A and D, were not designed to control the failure mechanism. Rather, they represent a baseline for performance of the more heavily detailed walls which were designed to have a flexural yielding mechanism. Walls B and E were intended to yield at the base level while the confined first course of Walls C and F was intended to shift the flexural yielding above this level. The double layers of reinforcing mesh at the top and bottom of each of these walls is designed to confine the compression zones of the wall and to avoid failure at the transition from the skins to the box beam and foundation. Provision of nail spikes in the header beams resists slip at this interface, to ensure a ductile mechanism can form.

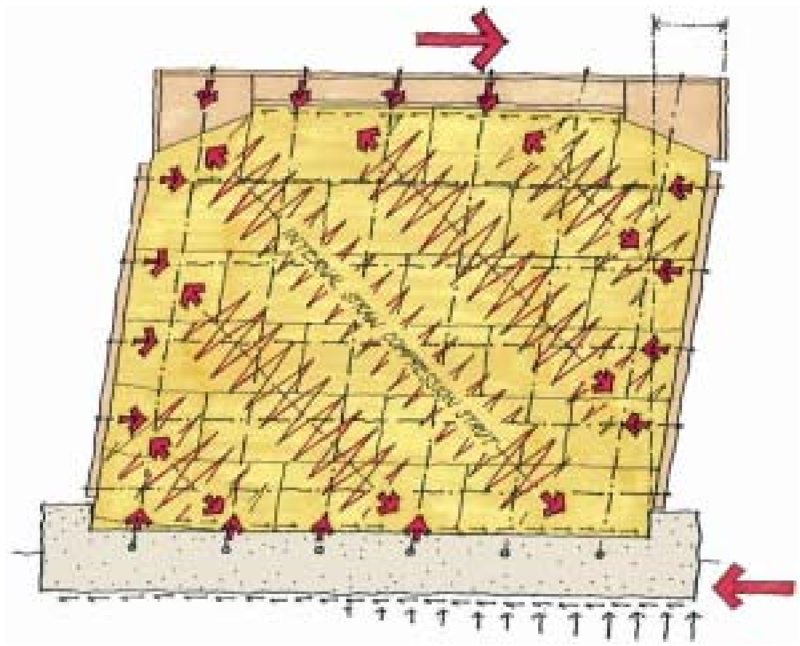

Figure 2.1 – Illustration of possible load path

## 3. Specimen Description and Fabrication

The following sections describe the materials and construction of the straw bale wall assemblies. Several of the terms used are specific to this type of construction and care has been taken to ensure their proper context or provide a definition.

### 3.1. Specimen Description

Six plastered straw bale assemblies were constructed and tested. Internally, each wall was similar, with six straw bale courses stacked in a running bond. Each course was the width of two bales, a nominal 8-foot width per course. The nominal height of each wall, from bottom of bale to top of bale, was also 8 feet. Two different skin materials, earth plaster and cement stucco, and three different levels of reinforcement details were used, representing light, medium, and heavy reinforcement. Reinforcing details were either selected from practical use or modified to obtain a desired result as discussed in Chapter 2. Some details are simple such as several twine tie-downs, while others are more complex such as lapped wire mesh and confined bale courses. Figures 3.1 through 3.6 show construction drawings for each of the six wall specimens.

### 3.2. Wall Construction

Wall construction began with the assembly of a wood base, comprised of 6×6 timbers in a horizontal ladder configuration, serving as a foundation and used for lifting and moving the wall specimens into the testing setup. Then, various mudsill configurations were constructed, according to the type and level of reinforcement desired. If specified, reinforcement (Walls C and F) or poly-twine (Wall A) was lapped under the mudsill. Wall A also required the driving of 16d nails into the mudsill, to reduce the likelihood of slip at this interface. The straw bales were then stacked on the base in a running bond, starting with two whole bales on the first course and one central bale bordered by two half bales on the second course. This pattern was repeated for the six courses comprising the 8-foot wall height. Where required (Walls B, C, E, and F) cross ties were inserted through the stacked bales, serving to hold the skin reinforcement against the bales and to reduce or eliminate the tendency for local buckling under compressive loading. For the two walls representing heavy levels of reinforcing detailing (Walls C and F), the first course of bales was clamped via 8-5/8" threaded rods bolted through 4 plywood plates and secured to the wood base.

A header beam, constructed from 4×4 rails and 2×4 cross members with plywood facings as indicated in the construction drawings, was then placed on top of the six straw bale courses. Four walls (A, B, C, and F) had header beams with 20d spikes driven through the bottom layers of plywood, serving as spikes to penetrate the top course of bales and increase the slip resistance at this interface. Prior to final installation of the reinforcing mesh, a weight simulating the dead load of expected roofing materials was applied to the header beam. Serving to pre-compress the straw bales and replicate field construction conditions, this weight equal to 200 pounds per linear foot of wall (1600 lbs. total) was left in place at least overnight until the reinforcing mesh was secured to the mudsill and the header beam. Various methods were used for securing the reinforcing mesh depending on the wall detail, including staples with different leg lengths and application at varying spacing. After securing the mesh, 10" reinforcing steel dowels (#4 bar size) were secured to the previously installed crossties. The dowels were installed in order to hold the reinforcing mesh tight against the bale surface.

Once the desired reinforcing details were in place, the stucco or plaster skins were applied. The first step in earth plaster application was the spraying of a scratch coat of slaked clay (clay which has been saturated for at least 24 hours) over the surface of the stacked bales. This process helps reduce the loose straw fibers and prepares the surface for the brown coats. Two brown coats were applied, at minimum intervals of two days to allow for curing. Each brown coat was scarified to generate grooves of approximately 1/8" to increase adhering of subsequent coats. The third application was a finish coat which was smoothed with a trowel to the desired finish.

Cement stucco application was similar to the earth plaster, however, with no scratch coat applied. Three coats of stucco were applied, but with a curing time of only one day between coats. In addition, due to the nature of the stucco material, there was no need to scarify the surface between coats. All walls had a total nominal thickness of 1 1/2" for all skins applied.

All walls were constructed, cured, and tested within the High Bay structures testing facility at the United States Army Construction Engineering Research Laboratory in Champaign, IL. The indoor facility had a controlled climate to be comfortable for human occupancy.

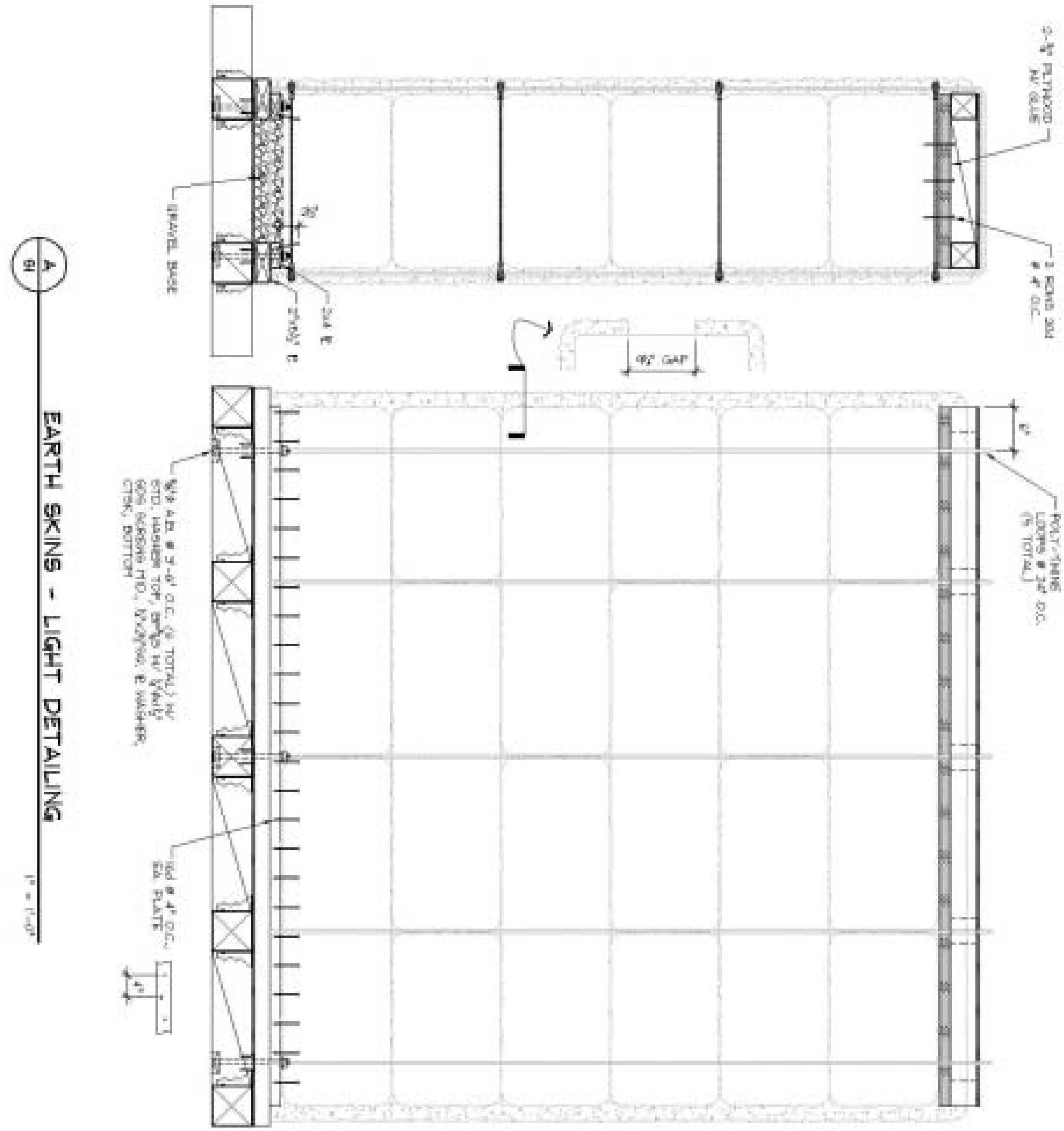


Figure 3.1 – Wall A

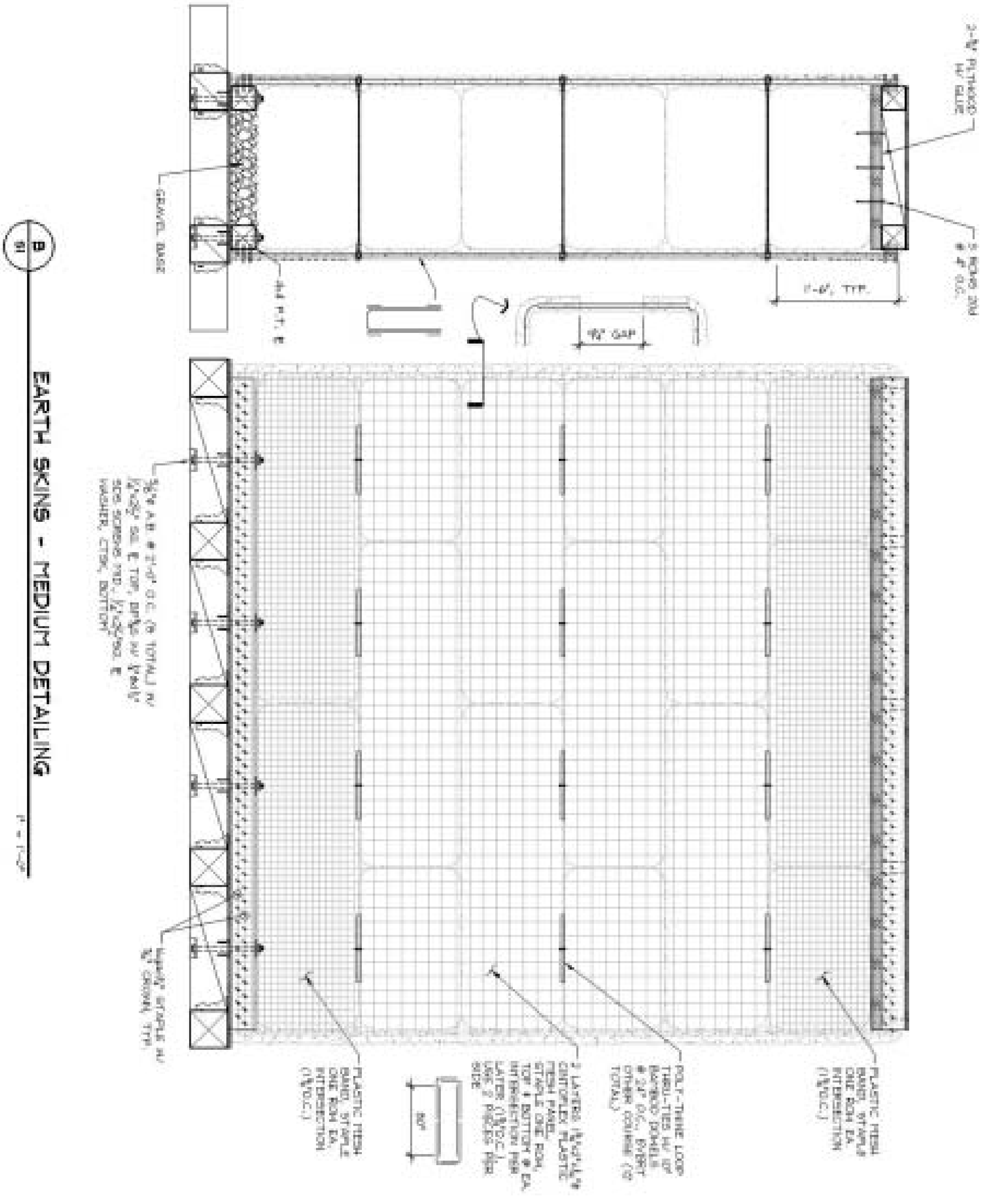


Figure 3.2 – Wall B

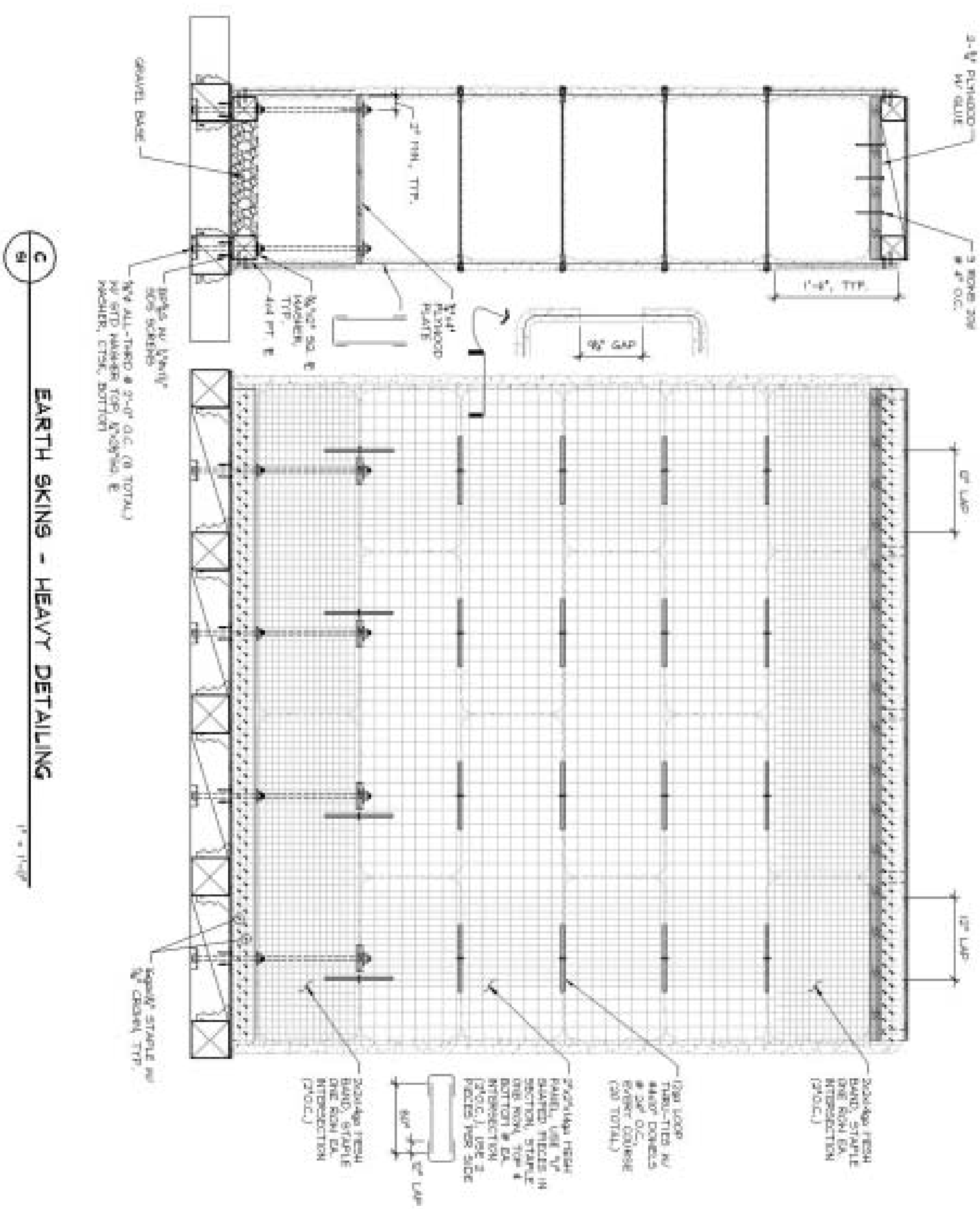


Figure 3.3 – Wall C

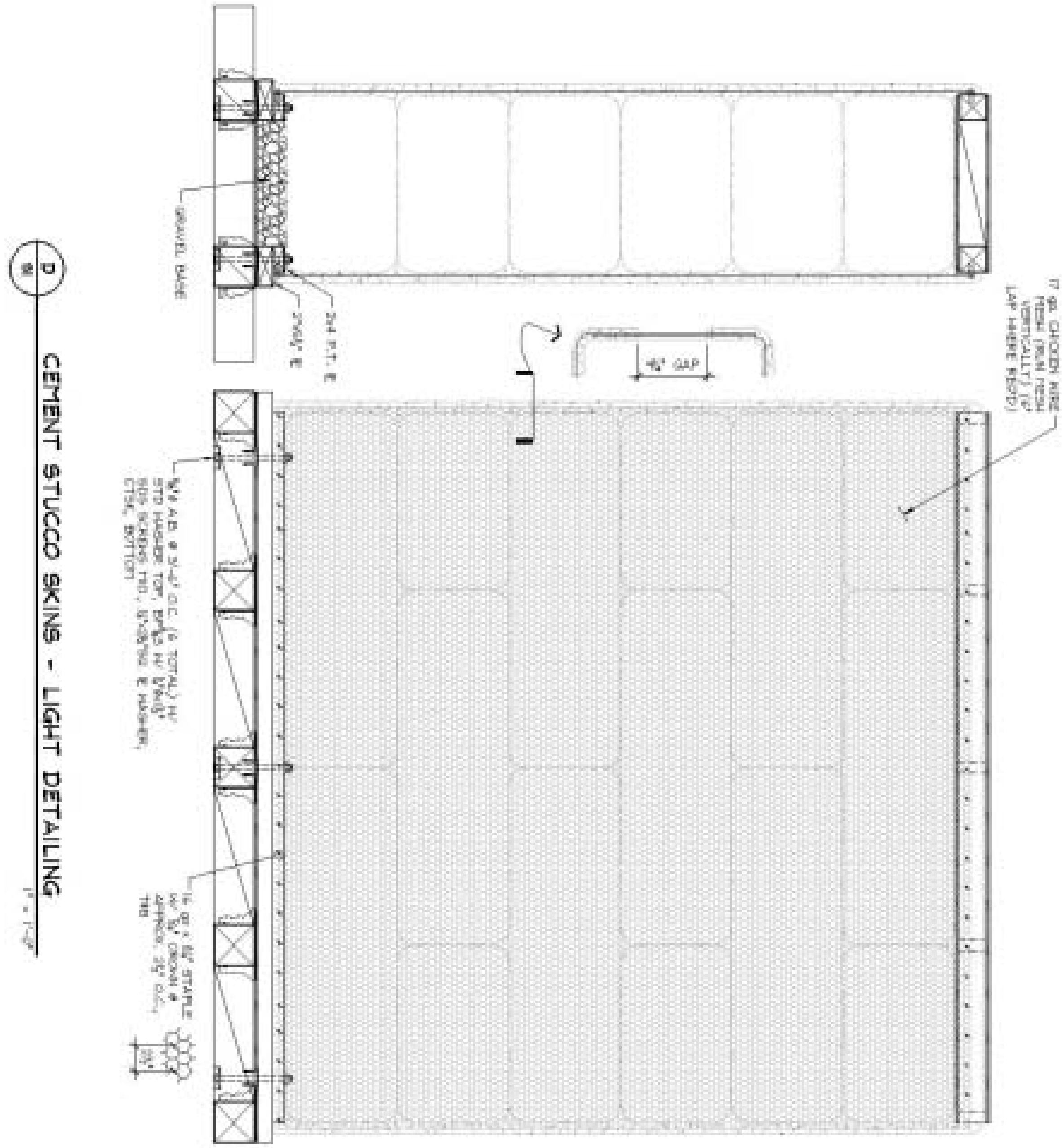


Figure 3.4 – Wall D

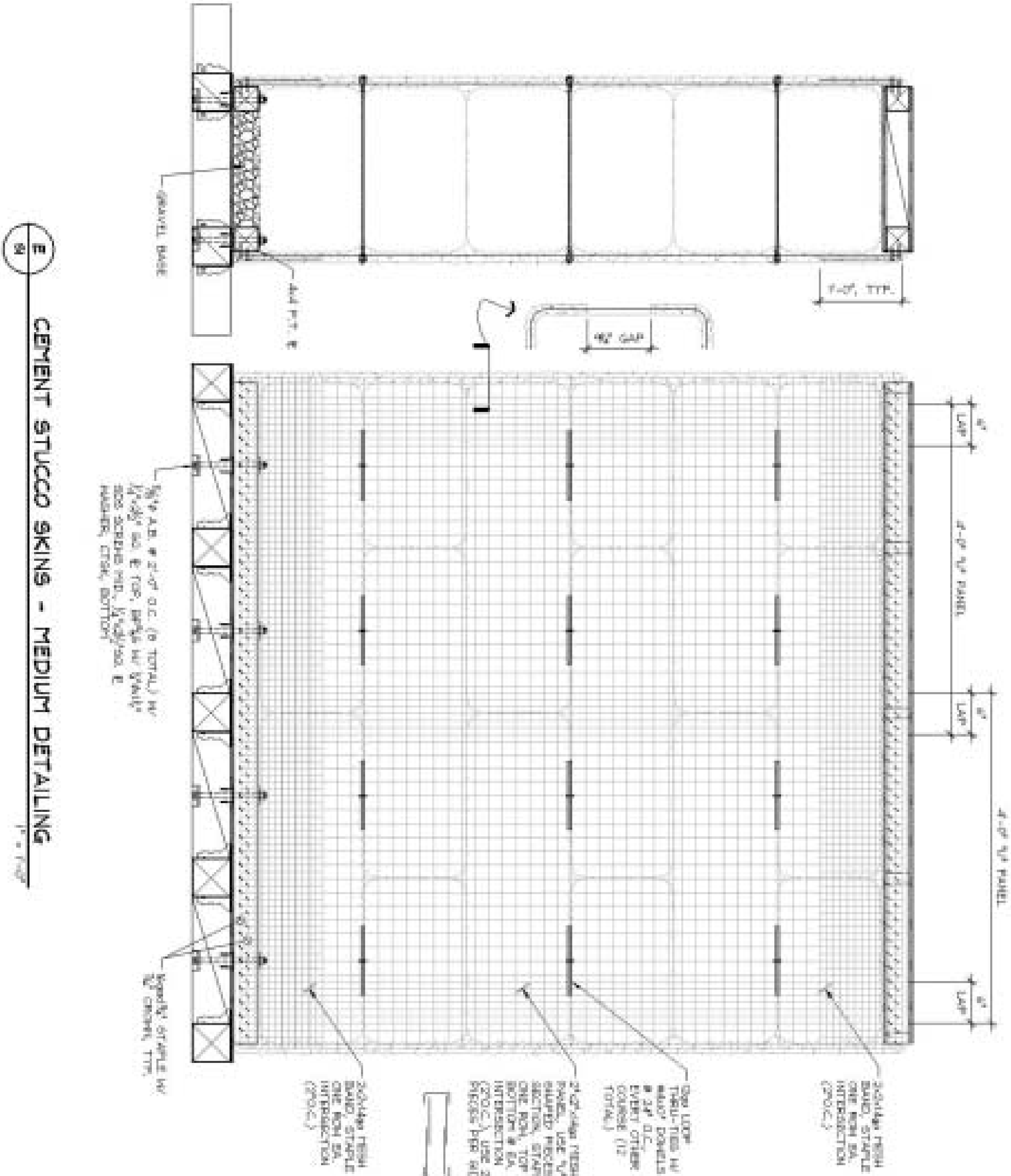


Figure 3.5 – Wall E

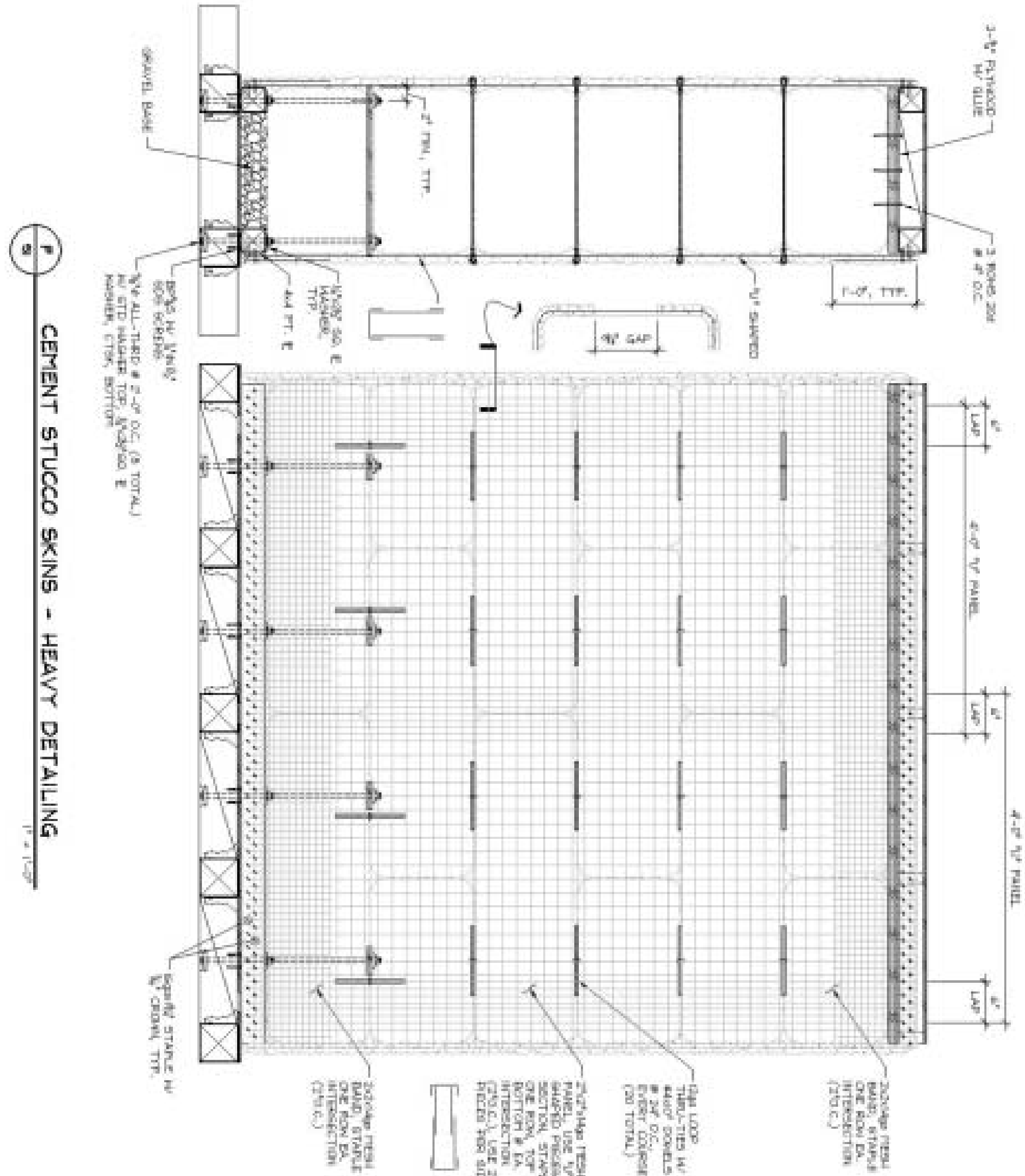


Figure 3.6 – Wall F

## 4. Materials

To every feasible extent, the construction of the six wall assemblies was conducted according to the "state of the practice" as it currently exists. Many of the materials used (straw bales, earth, welded wire mesh, and plastic mesh) were taken from their "usual" sources within California. The following sections describe the materials used in construction of the walls.

### 4.1. Straw Bales

The straw bales used were three-string rice straw bales having nominal dimensions of 16"×24"×48" (height, depth, width). The height and depth dimensions varied little from these values while the width (or length) had the greatest variance, due to the normal operation of the agricultural baling machines. The weights of the bales were measured at the time of construction and varied from 68 pounds to 85 pounds, illustrating the variation in density generated by the baling equipment.

### 4.2. Reinforcing Materials

One of the objectives of this experimental research project was to determine the impact of various reinforcing details and materials. As shown in Figures 3.1 – 3.6, several combinations of reinforcement and configuration were employed in the wall construction. In total, there were four types of skin reinforcing materials used:

- The lightly reinforced earth plaster wall, A, had five poly-twine loops running continuously over the header beam and under the 2×4 mudsill. The ploy-twine used was Farmland 350 lb. Baling Twine and is marketed as a replacement for bailing wire.
- The lightly reinforced cement stucco wall, D, used 17 gauge chicken wire mesh for reinforcement and to assist with stucco application. The roll width was 36".
- The medium reinforced earth plaster wall, B, used a black plastic mesh consisting of 0.05" nominal diameter legs on 1 7/8" center as reinforcement and it came on an 96" wide roll.
- The remaining three walls, C, E, and F, used a welded wire mesh consisting of 14 gauge wires intersecting at right angles every 2" on center and a roll width of 48".

### 4.3. Skin Materials

Two types of skin materials were used. Earth plaster and cement stucco represent two common alternatives for straw-bale construction. Both materials and described in the following sections, including information on compressive strength and strength gain. All compressive strength results were obtained following ASTM C 109-99 with a few modifications. The 2" cubes were tested with a displacement-controlled loading rate of 0.0015 in/s. Results are presented with the number of curing days noted. The curing periods recommended by ASTM C 109-99 were not always used; instead the cubes were tested at an early age and near the day of test to assess strength gain properties.

#### 4.3.1. Earth Plaster

Walls A, B, and C were constructed with earth plaster skins. Comprised of earth, sand, water and straw fibers, this natural plaster can be mixed partially from materials found on the construction site. However, to preserve field-learned techniques, clayey earth familiar to the construction crew was brought from California and used in preparing the earth plaster.

Compression tests yielded inconsistent results. One set of three samples had an average compressive strength of 290 psi after curing for 44 days while another set had an average of 160 psi after curing 94 days. The samples were prepared at different times from the same batch of earth plaster. This variability in strength results could be due to the heterogeneous properties of the natural materials used, or might possibly reflect changes in moisture content.

### 4.3.2. Cement Stucco

Walls D, E, and F were constructed with cement stucco skins. This stucco used Portland cement and lime as a binder, instead of clay in the earth plaster. Small batches were mixed in a mortar mixer in the following quantities: 30 gallons of sand, 8 gallons of cement, 2 gallons of slaked lime, and 6-1/2 gallons of water. The lime was hydrated prior to mixing by mixing in 6 gallons of water into a 50 pound bag of slaked finish lime. This was allowed to hydrate for five days until the lime ceased absorbing water.

Compressive test results for cement stucco were more consistent than for the earth plaster. At 7 days, a three cube set had an average strength of 1850 psi. At 36 days, three cubes from the same batch had an average strength of 2210 psi, while another set of three cubes from the same batch had a strength of 2200 psi at 95 days. The materials used in the cement stucco have better defined engineering properties, which was reflected in the consistency of the results.

### 4.3.3. Curing Environment

The earth and stucco plasters were applied to the walls and cured in the same environment as the cube samples. Temperature and relative humidity of laboratory were recorded periodically. The recorded values are shown in Figure 4.1, with a mean temperature of 70.7°F and a mean humidity of 41.7%.

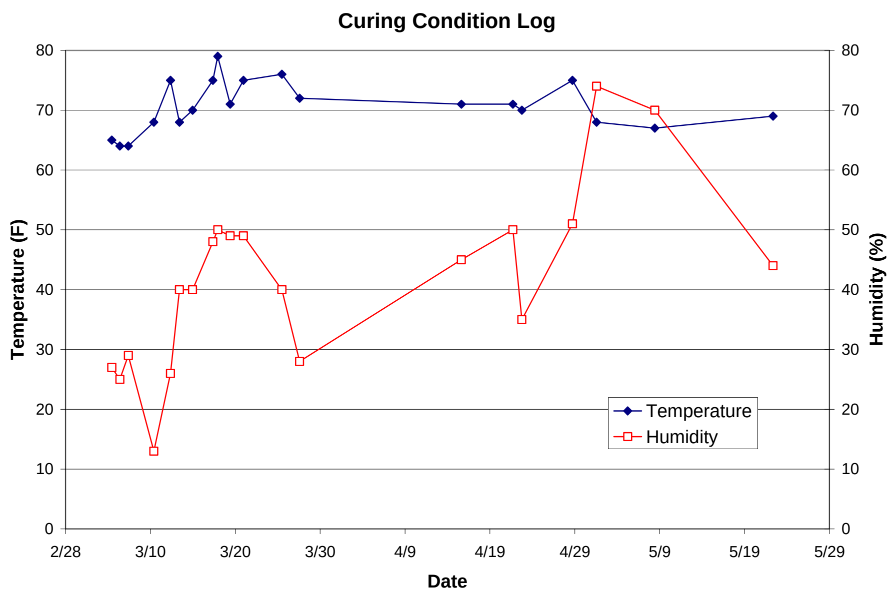


Figure 4.1 – Curing conditions

## 5. Experimental Testing Sequence

The experimental testing portion of the project followed the construction of the wall specimens. The following sections discuss the testing protocol and the testing sequence of the walls.

### 5.1. Testing Protocol

The test protocol provides an explicit set of instructions for the testing of a particular specimen. In this case, it provided displacement instructions to control the movement of the actuator at the top of each wall. All tests in this project were conducted in-plane, meaning that the forces are applied parallel to the 8' length of the wall. This method of load application is said to be against the strong axis of the wall and can be coupled with out-of-plane test results in predicting the response of a building. The test apparatus provided restraint against out of plane movement of the actuator and tube assembly at the top of the wall.

All walls with the exception of the lightly detailed earth plaster wall (Wall A) were tested according to the same protocol, described in the following section. Wall A was is not intended for seismic resistance but rather for non-seismic applications. Therefore, a cyclic testing protocol was too rigorous. A simple monotonic displacement profile was instead used as shown in Figure 5.1.

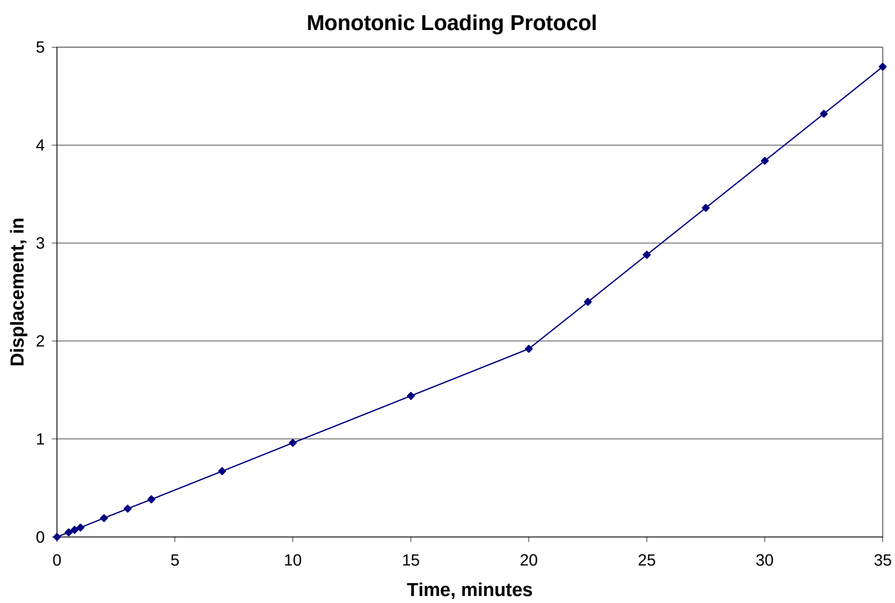


Figure 5.1 – Monotonic loading protocol

In order to gain sufficient data on the engineering properties of the other five straw bale wall assemblies tested cyclically, a protocol was desired which would not incur premature damage to the specimen. The protocol shown in Figure 5.2 was modified from an existing one used for testing shear walls and was deemed suitable for this application. Based on research and prior experience, initial yielding was expected to occur at perhaps 0.10% of the nominal wall height of 96". This cyclic displacement of 0.096" was selected as the third load step increment, occurring at 26.5 minutes after the test start. This predicted initial yield drift level was reached on the 14th cycle, providing many cycles of smaller amplitude data on the elastic properties of the tested wall. As shown in Figure 5.2, there are many cycles in the small displacement range to capture the yielding behavior of the tested wall. Subsequent cycles increase in amplitude, reaching 5% drift (4.80 in) at the end of the protocol.

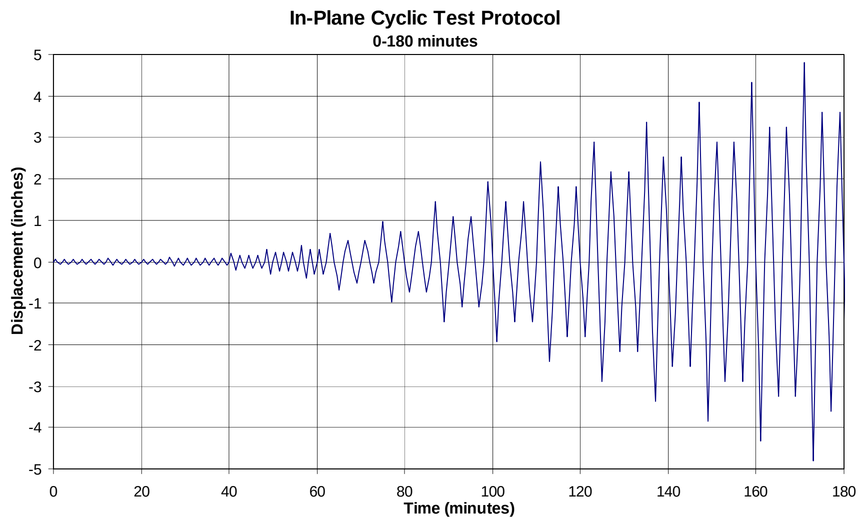


Figure 5.2 – Cyclic test protocol (0-180 minutes)

This protocol has 16 load steps of increasing displacement with trailing cycles after each peak cycle as shown in Table 5.1. After completion of the programmed test protocol, each wall was manually loaded to obtain two cycles of 7.5% drift (7.2 in). This extreme displacement was used to establish the performance of the straw ball wall assembly at high drifts. Higher drifts could not be obtained due to physical limitations of the testing setup.

Table 5.1 – Cyclic protocol information

| Load Step | Drift | Peak Displacement | Trailing Cycle Disp. | # of Trailing Cycles |
|---|---|---|---|---|
| 1 | 0.050% | 0.048 | 0.048 | 5 |
| 2 | 0.075% | 0.072 | 0.054 | 6 |
| 3 | 0.100% | 0.096 | 0.072 | 6 |
| 4 | 0.20% | 0.192 | 0.144 | 3 |
| 5 | 0.30% | 0.288 | 0.216 | 3 |
| 6 | 0.40% | 0.384 | 0.288 | 3 |
| 7 | 0.70% | 0.672 | 0.504 | 2 |
| 8 | 1.00% | 0.960 | 0.720 | 2 |
| 9 | 1.50% | 1.440 | 1.080 | 2 |
| 10 | 2.00% | 1.920 | 1.440 | 2 |
| 11 | 2.50% | 2.400 | 1.800 | 2 |
| 12 | 3.00% | 2.880 | 2.160 | 2 |
| 13 | 3.50% | 3.360 | 2.520 | 2 |
| 14 | 4.00% | 3.840 | 2.880 | 2 |
| 15 | 4.50% | 4.320 | 3.240 | 2 |
| 16 | 5.00% | 4.800 | 3.600 | 2 |

## 5.2. Testing Sequence

Due to the nature of the skin materials, cement stucco and earth plaster, a curing period was required before testing could begin. A four-week curing time was deemed suitable for the cement stucco skinned walls (D, E, and F) while an eight-week curing time was recommended for the earth plaster skinned walls (A, B, and C). This curing requirement allowed the cement stucco skinned walls to be tested while the earth plaster skinned walls (which were constructed first) continued curing.

Prior to testing, each wall specimen had to be lifted and moved into the test setup. Strong-back lifting rails were bolted through the 6×6 cross rails for overhead crane lifting in order to minimize bending distortions to the wall. The test setup was equipped with a flat 3’×11’ stiffened steel plate for securing the base of the wall. Each wall was placed on a bed of hydrocal (quick-setting gypsum cement) on top of the steel plate to provide an even bearing surface. Once the hydrocal had set, the wall was released from the crane and ten 7/8” bolts and twelve 3/4”×4” lag screws were used to securely fasten the base of the wall to the steel plate, which was in turn anchored to the laboratory strong floor. Two shear blocks were installed at each end of the wall and hardwood shims were driven into this gap to minimize potential base slippage during loading. The header beam at the top of each wall was fastened to the loading beam via 3/4”×4” lag screws installed through angles bolted to the tube and into the 4×4 rails of the header beam. The resulting dead load on the top of each specimen was adjusted to provide nominal values of 200 pounds/linear foot or 1600 pounds total by use of a pulley and weight system attached to the loading tube. After installation, the exposed wall surface was whitewashed with a mixture of finish lime and water to provide an even background for photography and to assist in the identification of cracks and crack growth.

As mentioned in the previous section, all walls with the exception of the lightly detailed earth plaster wall, which was tested monotonically, were tested with the same cyclic test protocol. Occasional pauses were taken to mark crack growth and document structural behaviors. Thorough graphic documentation in the form of time-lapse and full motion videos and still photographs of details was obtained and is referred to in the test results section.

### 5.3. Instrumentation

In order to capture the structural response of each wall tested, several measurements were taken using precision instrumentation devices. The measurements taken can be divided into two main groups, overall structural response and more detailed wall response.

Overall structural response can be considered the first-order description of the wall response and includes the measurements taken from the loading actuator, load and displacement. These results can be plotted in a load versus displacement format, useful for comparing the gross performance characteristics of each specimen.

Additional instrumentation was used to further evaluate the structural response and effectiveness of various details. Cost, complexity, and fidelity are all considerations when designing an instrumentation setup. Prior research and experience combined with some engineering judgment led to the design of the instrumentation shown in Figure 5.3, which uses cable-extension transducers (CETs) for measuring the displacement of Points A, B, C, and D. Each CET converts the extension of a flexible cable into a voltage which is digitally recorded at a rate of 2 hertz. These voltage measurements can be converted to displacement during subsequent data analysis.

In total, seven CETs were used in two arrays. CET Array 1 had three transducers and Array 2 had four (Figure 5.4 shows Array 2 for reference). Each array was attached with the 3/4”×4” lag screws fixing the header beam to the loading beam, maintaining a constant distance between the arrays. CETs 1 and 4 measured the spatial displacement of Point A, CETs 2 and 5 measured Point B, CETs 3 and 6 measured Point C and Point D was measured by CET 7 alone. Points C and D were rigidly attached to the 6×6 wood base, with a constant spacing, and measure the overall deformations of the wall. Points A and B were inserted in small holes drilled into the plaster material, and measure interstitial deformations within the wall. Point A was located just below the start of the third bale course and Point B was located just below the second bale course, in order to measure the deformation in each course.

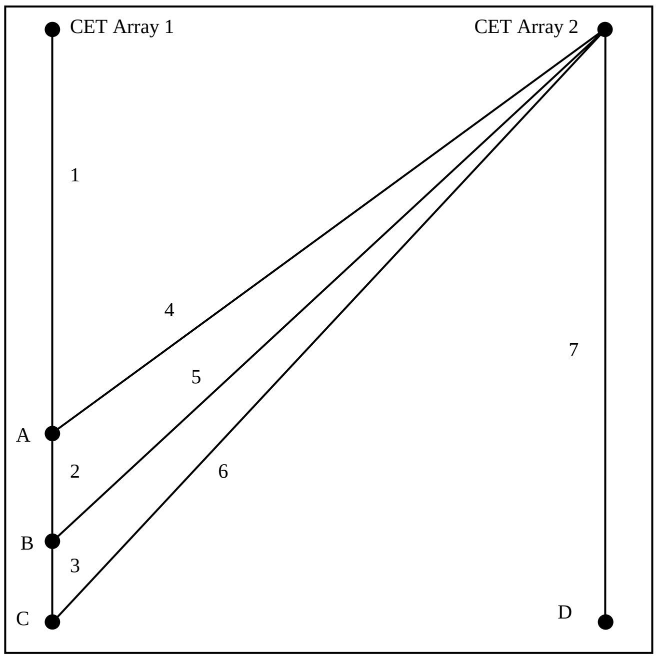

Figure 5.3 – Instrumentation schematic


Figure 5.4 – Cable-extension transducer array photograph (transducer circled)

## 6. Test Results

The following sections contain a detailed description of the behavior and performance of each wall assembly tested. The results are presented in alphabetical order, not reflecting the order in which they were tested nor their performance.

### 6.1. Wall A – Earth Plaster Skins with Light Detailing

Inspection of the Wall A prior to loading revealed the earth plaster to have pulled away from the box beam while drying, leaving visible gaps of 1 to 2 inches between the plaster and box beam around approximately half of the perimeter of the box beam, perhaps due to the lack of mesh reinforcement for the plaster to adhere to.

Wall A was not designed to resist seismic actions and was therefore tested under monotonic loading. The loading was carried out at a rate similar to the initial rate of the cyclic protocol, and pauses were taken at each of the peak displacement values given in Table 5.1 to observe and record the progression of damage to the wall. The resulting load-displacement plot is shown in Figure 6.1. One may observe a minor reduction in load at each pause.

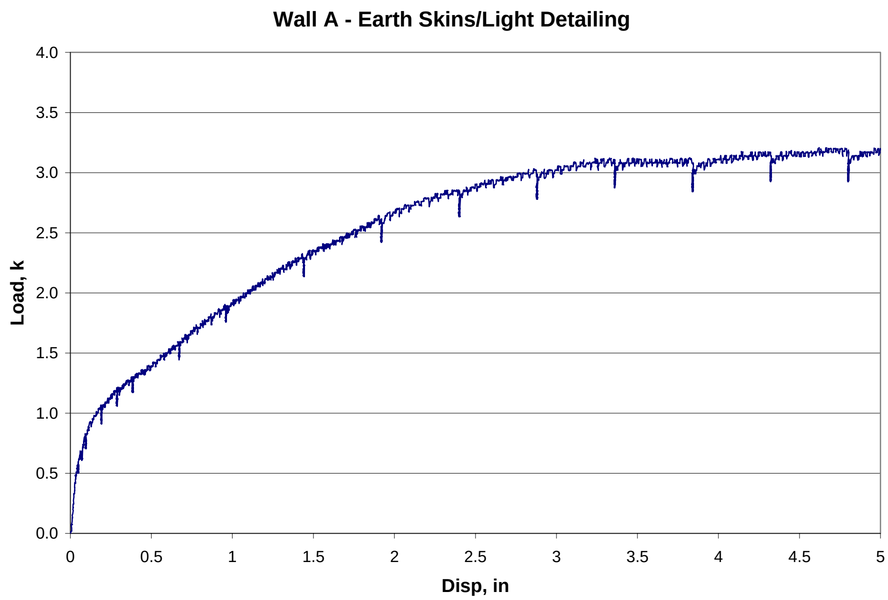


Figure 6.1 – Wall A load-displacement plot

The peak capacity of Wall A was 3.2 kips, which was reached at 4% drift (3.84 inches) and was maintained for higher displacements. Non-linear load-displacement response was observed near 0.75% drift and a load of 0.7 kips. However, the load capacity continued to increase up to 3.5% drift and remained constant after this. During loading, the header beam was observed to slip relative to the top course of bales as evidenced by cracking in the plaster returns at the top of the wall as shown in Figure 6.2. At lower displacements (less than 2.4 inches) the failure mode appeared to be dominated by slip of the box beam relative to the top course of bales, corresponding to lateral loads less than 2.85 kips. Above this 2.5% drift level, crushing of the earth plaster in the compression zone commenced as lateral load capacity increased to the maximum value of 3.2 kips. The increase in lateral resistance and shift in location of damage suggests that the poly-twine loops around the box beam became engaged after the box beam slipped sufficiently. There was no evidence to suggest the poly-twine failed at any point during the tests, as the poly-twine was found to be taught when inspected at the gaps that opened at the base of the wall during testing.

Figure 6.2 – Evidence of header beam slippage in Wall A

**6.2. Wall B – Earth Plaster Skins with Medium Detailing**

Wall B was designed and built with a plastic reinforcing mesh. While not as stiff or strong as the 2”×2” wire mesh, this plastic mesh provided additional skin reinforcement relative to that in Wall A. A side benefit to using some form of mesh is that the plaster has something to bond to, reducing or avoiding the peeling problems of Wall A, which had no mesh reinforcement.

During testing, the predominant failure mode observed was compression zone crushing and base sliding, with the base sliding becoming more pronounced at later stages of the test. The peak capacity of 4.7 kips was reached on the $8^{th}$ load step, at a drift level of 1% (0.96 inches). Looking at the load-displacement plot in Figure 6.3, the change in the hysteresis loops with increasing displacements suggests that sliding of the wall becomes more significant at higher displacements. Manual measurements taken to assess the sliding behavior indicated 3/4” amplitude (peak to peak) of slip during load step 14 (4% drift), accounting for 20% of the actuator displacement at this amplitude. The higher amplitude cycles were observed to wear down the earth plaster at the base, which gradually reduced it to sand, clay, and straw components, resulting in a corresponding reduction in the height of the wall, due to this wearing and crushing behavior. Often this soil debris served as a wedge to push the plaster out of plane, away from the bales, when the plaster was loaded in compression. As this occurred, the plaster would crush down over the 6×6 ties, thereby creating a form of interlock and shear resistance that might not be available in practical, non-laboratory settings. However, this behavior began only after drifts of 2.5%.

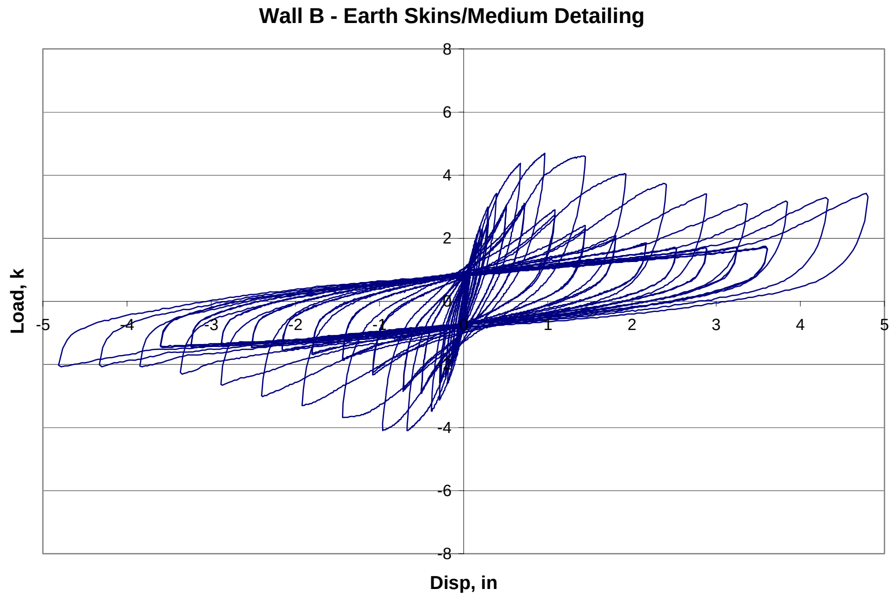


Figure 6.3 – Wall B load-displacement plot

### 6.3. Wall C – Earth Plaster Skins with Heavy Detailing

Wall C used a heavy 2”×2” 14-gauge wire mesh with the first course of bales anchored to the base via plywood plates and threaded rods. As shown in Figure 6.4, these modifications resulted in an increase in the lateral strength of this wall relative to that of Wall B, with a peak load of 6.1 kips occurring at 1.5% drift (1.44 inches). At 1% drift, the 6.0 kip resistance was an increase of nearly 30% over the corresponding resistance of Wall B at this drift level.

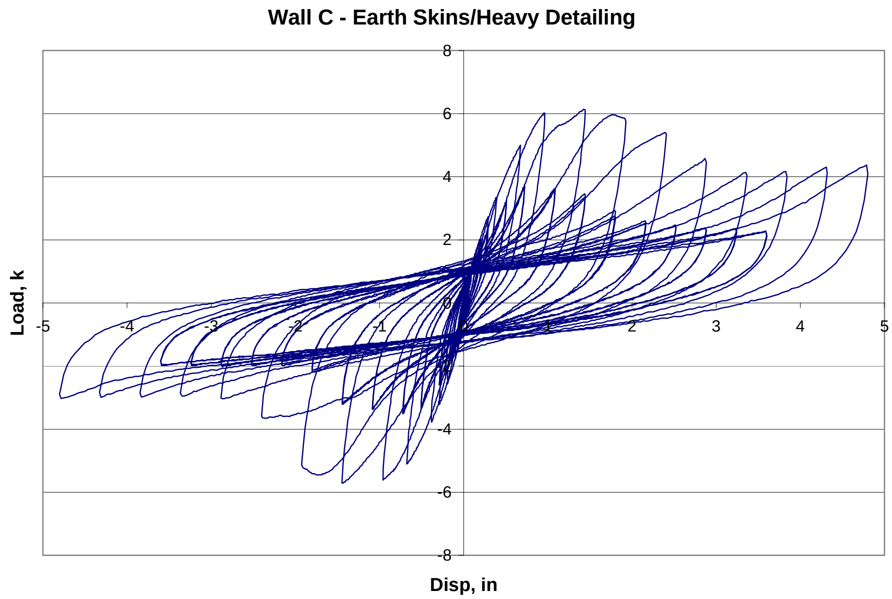


Figure 6.4 – Wall C load-displacement plot

The overall structural response of this wall was similar to that of Wall B, with predominant failure modes consisting of crushing of the earth plaster and sliding of the wall at its base. The heavier mesh was observed to reduce the slip at the base of Wall C from a peak-to-peak amplitude of 3/4” in Wall B to 1/2” amplitude in this specimen at a drift of 4%. No flexural tension cracks were observed during testing of Wall C, indicating the mismatch of plaster compressive strength to wire mesh tensile strength. Similar to Wall B, this wall also experienced the plaster interlocking with the 6×6 ties at drifts above 3%.

### 6.4. Wall D – Cement Stucco Skins with Light Detailing

The lightly detailed cement stucco wall used 17-gauge chicken wire mesh as skin reinforcement and to assist stucco placement. Unlike Wall C, this combination of a strong skin and a relatively weak reinforcement led to a different failure mode. The initial stiffness of the walls with cement stucco skins was greater than that of the earth plaster skins. Figure 6.5 shows the load-displacement plot for this test and the pinching nature of the hysteresis loops suggests the presence of the rocking behavior that was visually observed at higher displacements.

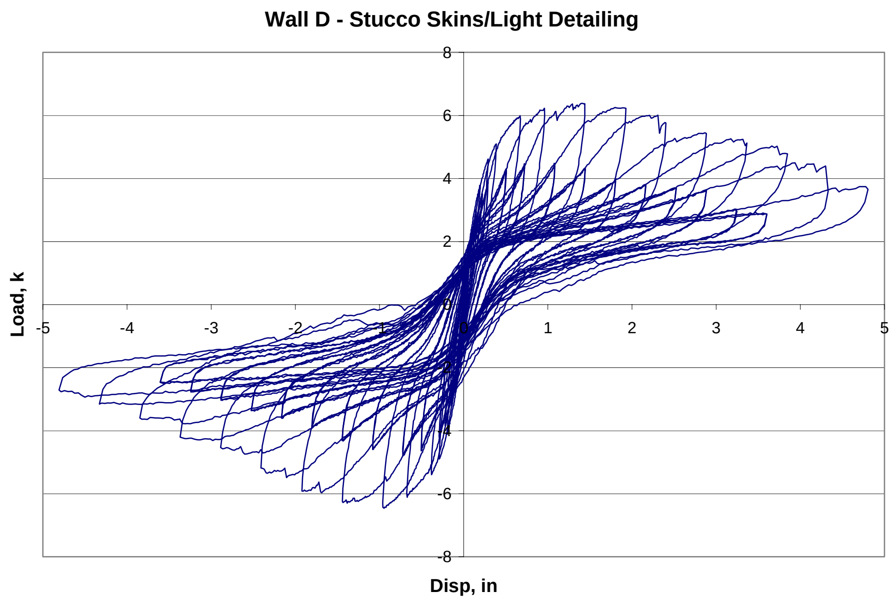


Figure 6.5 – Wall D load-displacement plot

The peak load of 6.4 kips was only marginally higher than that observed for Wall C, but the post-peak behavior was dominated by rocking rather than sliding. As higher displacements were reached, two distinct failures were observed at the base of the wall. In some locations the weak mesh was elongated and had fractured, while at other locations the 2×4 sill plate receiving the mesh staples failed in cross-grain bending as shown in Figure 6.6. By the end of the test, the combination of mesh fractures and sill failure had progressed along the full length of the wall, allowing the observed rocking behavior to occur unimpeded. None of the staples anchoring the mesh were observed to fail or pull out.

Figure 6.6 – Wall D cross-grain bending failure of sill plate
(Photographed at 5% drift, well after failure had occurred)

**6.5. Wall E – Cement Stucco Skins with Medium Detailing**

For the medium-detailed cement stucco wall the heavier 14-gauge 2”×2” mesh was used to reinforce the stucco and additional staples were used to attach the stucco to both the sill plate and the header beam. Through-ties running through the thickness of the wall and anchored by dowels in the body of the stucco were installed at every other course, to reduce the likelihood of skin buckling under compressive loading. Instead of the 2×4 sill plate, which failed in Wall D, a 4×4 sill plate was used, and the 4×4 plate was anchored more frequently. The combination of cement stucco skins and heavier wire mesh resulted in an increased lateral strength, having a peak value of 19 kips at 2% drift, as shown in Figure 6.7.

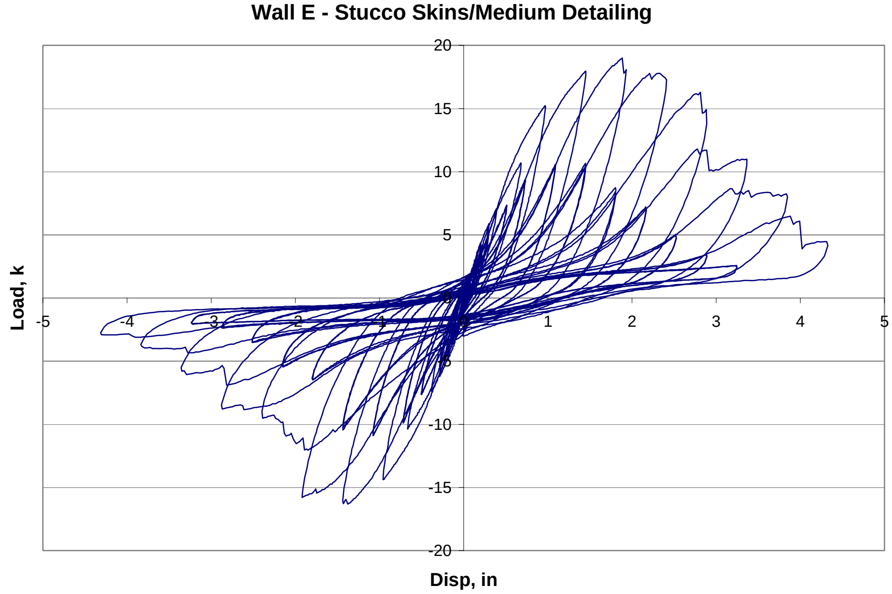

Figure 6.7 – Wall E load-displacement plot

This increase of nearly 200% over Wall D was associated with the development of several flexural cracks within the bottom third of the wall height as shown in Figure 6.8. The ultimate failure mode for Wall E was the loss of tensile capacity of the reinforcing mesh, from both mesh fracture and staple pull out, as shown in Figure 6.9. The mesh fracture was attributed to a combination of tensile elongation and low-cycle fatigue associated with the load reversals, which appeared to work the vertical wires of the mesh. The failures predominately occurred at the staple locations with some failures also occurring at the intersections of the horizontal and vertical wires, where the wires are spot welded together in the manufacturing of the mesh.

Figure 6.8 – Flexural cracks in Wall E (2.5% drift level)

Figure 6.9 – Wall E mesh failure (7.5% drift level)

### 6.6. Wall F – Cement Stucco Skins with Heavy Detailing

The heavily detailed Wall F added spikes from the header beam, additional cross ties, and confinement to the first bale course to the details of Wall E. Figure 6.10 shows the load-displacement response of this wall. The peak lateral strength of 18.2 kips was reached at 1.5% drift, and the capacity at 2% drift was 17.9 kips. A comparison of Figures 6.7 and 6.10 from Walls E and F, respectively, shows the limited benefit gained from the additional detailing provided in this wall.

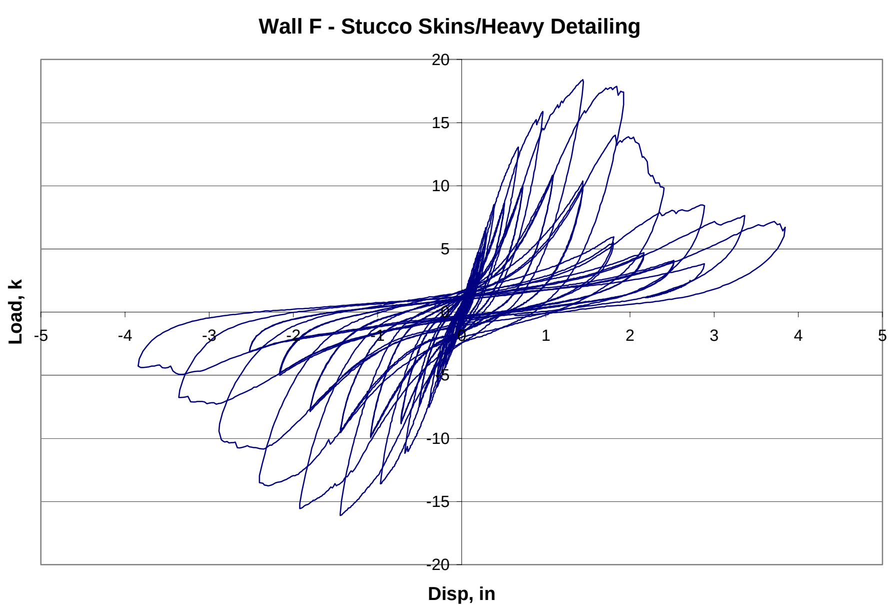


Figure 6.10 – Wall F load-displacement plot

The confinement of the first bale course was intended to shift the failure above this level while distributing the yielding of the reinforcing mesh over more of the wall height, aiming to achieve a more ductile behavior. The ultimate failure was indeed observed at this level as shown in Figure 6.11, although there was not an appreciable difference in the ductility or strength of this wall compared to Wall E.


Figure 6.11 – Wall F flexural cracks (2.5% drift level)

## 7. Discussion of Test Results

The results presented in Chapter 6 are compared and discussed in the following two sections. Comparisons to the predicted wall behavior are made in the third section.

### 7.1. Relative Performance of Earth Plaster Skinned Walls

A comparison of the three earth plaster skinned walls tested is shown in Figure 7.1. As this plot indicates, the added reinforcement of Wall C did increase the capacity over that of Wall B across the entire displacement range. The monotonically tested specimen, Wall A, had a capacity similar to that of Wall B at higher displacements (over 3 inches) but a lower capacity in the smaller displacement range. All three walls performed acceptably in the higher displacement ranges, with no indications of instability.

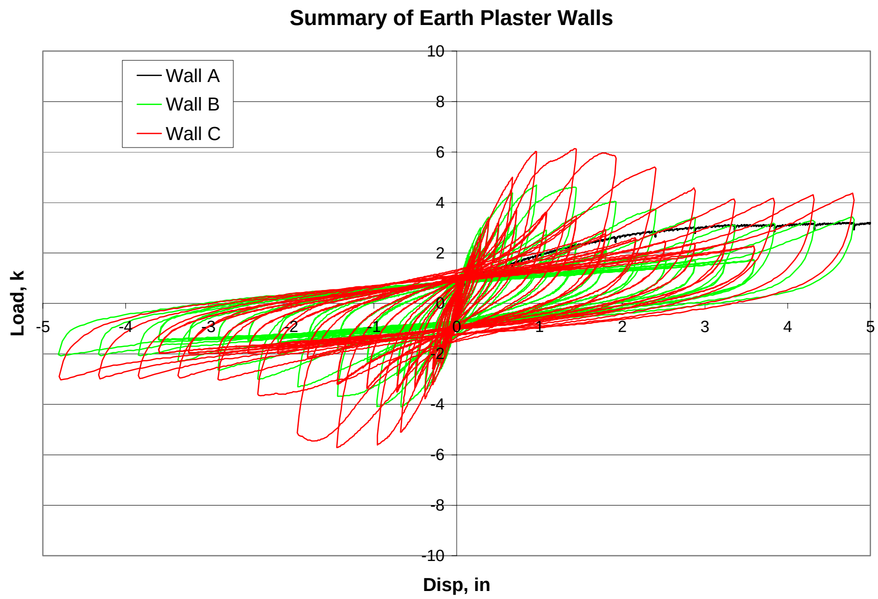


Figure 7.1 – Summary of earth plaster wall tests

### 7.2. Relative Performance of Cement Stucco Skinned Walls

Overall, the cement stucco skinned walls had higher capacities than the correspondingly detailed earth plaster skinned walls. As shown in Figure 7.2, both strength and stiffness are increased relative to Walls A, B, and C. The lightly detailed cement stucco specimen, Wall D, had only a small increase in capacity over the heavily detailed earth plaster specimen, Wall C. However, Walls E and F had substantially higher capacities than any of the other four specimens. The individual capacities of these Walls E and F were nearly identical as illustrated by the oft-overlapping curves in Figure 7.2. Similar to the earth plaster walls, all three cement stucco walls performed acceptably at higher displacements. For all specimens, the strength capacities above 4% drift (3.84 inches) were similar.

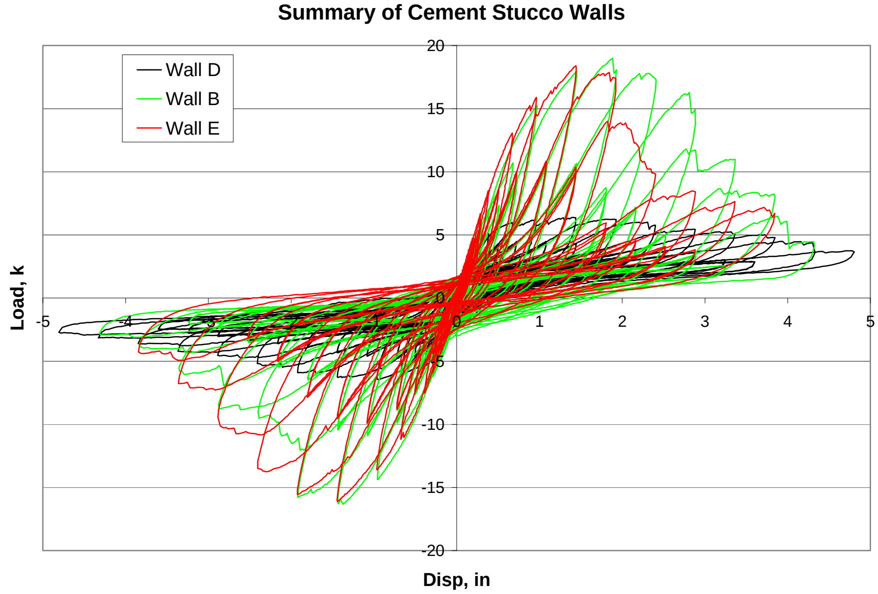


Figure 7.2 – Summary of cement stucco wall tests

**7.3. Comparison to Predicted Mechanisms**

Chapter 2 identified the intended mechanism for each wall tested. As mentioned, Walls A and D had no intended control over their behavior. Wall A experienced sliding at the header beam and at the base level while Wall D experienced rocking after failure of its weak reinforcing mesh. The remaining four walls were detailed to control the resulting mechanism. Walls E and F were able to obtain flexural yielding behavior, ultimately fracturing the reinforcing mesh and then rocking. Walls B and C were unable to obtain flexural yielding due to the low compressive strength of the earth plaster skin. Rather, these walls experienced crushing of the compression zone, which mobilized the straw as a vertical compression strut, and sliding at the base.

**8. Conclusions and Recommendations**

Based on the preceding discussions, several conclusions can be made:

- The material properties of the cement stucco appear to be better defined than for the earth plaster
- The lack of reinforcing mesh in Wall A lead to lower capacity and problems with plaster adhesion to the box beam at the top of the wall
- Ductile tension failures were obtained only with the cement stucco skinned walls
- All walls displayed stable response at high drift levels (5 and 7.5%) with no indications of collapse imminent
- The additional labor required for detailing Wall F resulted in no appreciable performance enhancement relative to Wall E

Coupled with these results are recommendations for future research.

- Additional material testing for earth plaster is desired to better characterize material properties such as compressive strength and strength gain
- More thorough component testing of reinforcing materials

The results from these recommended studies are required for a better comparison of predicted and measured wall capacity.